Eur Radiol (2009) 19: 358–369
DOI 10.1007/s00330-008-1166-8

ULTRASOUND

Man-Xia Lin
Hui-Xiong Xu
Ming-De Lu
Xiao-Yan Xie
Li-Da Chen
Zuo-Feng Xu
Guang-Jian Liu
Xiao-Hua Xie
Jin-Yu Liang
Zhu Wang

Diagnostic performance of contrast-enhanced ultrasound for complex cystic focal liver lesions: blinded reader study

Received: 2 May 2008
Revised: 4 August 2008
Accepted: 6 August 2008
Published online: 16 September 2008

M.-X. Lin · H.-X. Xu (✉) · X.-Y. Xie · L.-D. Chen · Z.-F. Xu · G.-J. Liu · X.-H. Xie · J.-Y. Liang · Z. Wang
Department of Medical Ultrasonics, The First Affiliated Hospital, Institute of Diagnostic and Interventional Ultrasound, Sun Yat-Sen University, 58 Zhongshan Road 2, Guangzhou, 510080, China
e-mail: xuhuixiong@hotmail.com
Tel.: +86-208-7765183
Fax: +86-208-7765183

M.-D. Lu (✉)
Department of Hepatobiliary Surgery, The First Affiliated Hospital, Sun Yat-Sen University, 58 Zhongshan Road 2, Guangzhou, 510080, China
e-mail: lumd@21cn.com
Tel.: +86-208-7765183
Fax: +86-208-7765183

Abstract The study was aimed at evaluating the diagnostic performance of contrast-enhanced ultrasound (CEUS) in characterizing complex cystic focal liver lesions (FLLs). Sixty-seven complex cystic FLLs in 65 patients were examined with conventional ultrasound (US) and real-time CEUS. The US and CEUS images were reviewed by a resident radiologist and a staff radiologist independently. Receiver operating characteristic (ROC) analysis was performed to evaluate the diagnostic performance, and the interobserver agreement was analysed. The results showed that complete non-enhancement throughout three phases of CEUS or sustained enhancement in the portal and late phases were exhibited in most benign lesions. Conversely, hypo-enhancement in the late phase was seen in all malignancies. After ROC analysis, the areas (Az) under the ROC curve were 0.774 at US versus 0.922 at CEUS (P=0.047) by the resident radiologist, and 0.917 versus 0.935 (P=0.38) by the staff radiologist. A significant difference in Az between the resident and the staff radiologists was found for US (0.774 versus 0.917, P=0.044), whereas not found for CEUS (0.922 versus 0.935, P=0.42). Interobserver agreement was improved after CEUS (κ=0.325 at US versus κ=0.774 at CEUS). Real-time CEUS improves the capability of discrimination between benign and malignant complex cystic FLLs, especially for the resident radiologist.

Keywords Complex cystic focal liver lesion · Contrast-enhanced ultrasound · Diagnostic performance · Receiver operating characteristic analysis · Interobserver agreement

Introduction

Complex cystic focal liver lesions (FLLs) are those FLLs containing large fluid-filled areas within the lesions; they are increasingly common in clinical practice as a result of the increasing use of hepatic imaging. Complex cystic FLLs represent a wide spectrum of liver lesions that include both benign and malignant lesions. Discrimination between benign and malignant complex cystic FLLs is of paramount importance since the management and prognosis vary greatly. Conventional ultrasound (US) has low ability in differentiating diagnosis between them [1–3] and the patients usually have to be referred to other imaging modalities such as contrast-enhanced computed tomography (CECT) or contrast-enhanced magnetic resonance imaging (CEMRI) for further characterization.

The development of low acoustic power contrast-enhanced ultrasound (CEUS) allows real-time depiction of dynamic blood flow perfusion throughout vascular phases and it has been documented that real-time CEUS greatly improves the diagnostic ability in characterization of FLLs [4–7], whereas few data were available with regard to CEUS in characterization of complex cystic FLLs. The present study was aimed to evaluate the diagnostic performance of CEUS for complex cystic FLLs.

Materials and methods

Patients

From March 2004 to October 2007, 67 lesions in 65 patients with complex cystic FLLs who had undergone CEUS in our institution were enrolled in this study. The patients were 35 men and 30 women, with a mean age ± SD of 46.4±15.4 years (range, 18–76 years). The inclusion criteria were: (1) showing anechoic portion on US; (2) confirmed by pathology or clinical information. Sixty-three patients had one lesion in each and the remaining two had two lesions in each. Among the 67 lesions, 35 were confirmed by histopathologic examination with specimens obtained from US-guided percutaneous biopsy (n=1) or surgical resection (n=34), 28 abscesses and one biloma were confirmed by US-guided aspiration or drainage, one hepatic cyst was confirmed by US-guided aspiration and follow-up, and the remaining two hematomas were confirmed by clinical data (i.e., history of liver trauma or surgery; evidence from other imaging modalities; disappearance of the lesion in follow-up) (Table 1). The maximal diameters of the lesions ranged from 2.0 to 14.9 cm (mean, 7.5± 3.0 cm). Written informed consent was obtained from all patients, and the study was approved by the Ethical Committee of the institution.

The final diagnoses of the lesions included 51 benign and 16 malignant lesions. They were pyogenic abscess in 29, hepatic cyst in five (complicated with intracystic hemorrhage in four), haemangioma in five, hematoma in four, cystadenoma in two, intrahepatic cystic cholangiectasis in one, cyst-like lesion in one, parasitic liver cysts in one, vascular hemangioma in one, infectious granuloma-like lesion in one, biloma in one; hepatocellular carcinoma (HCC) in six, liver metastasis in three (from nasopharyngeal carcinoma in one; from malignant ileac stromal tumor in one; unknown in one), cystadenocarcinoma in three, intrahepatic cholangiocarcinoma in two, combined hepatocellular and cholangiocarcinoma in two.

Table 1 Confirmed methods of complex cystic FLLs in this study (*HCC* hepatocellular carcinoma, *ICC* intrahepatic cholangiocarcinoma)

Entity	Histopathologic examination			Clinical data
	Surgical resection	Biopsy	US-guided aspiration or drainage	
Abscess (n=29)	1	0	28	0
Hepatic cyst (n=5)	4	0	1	0
Hemangioma (n=5)	5	0	0	0
Hematoma (n=4)	2	0	0	2
Cystadenoma (n=2)	2	0	0	0
Intrahepatic cystic cholangiectasis (n=1)	1	0	0	0
Cyst-like lesion (n=1)	1	0	0	0
Parasitic liver cysts (n=1)	1	0	0	0
Vascular hemangioma (n=1)	1	0	0	0
Infectious granuloma-like lesion (n=1)	0	1	0	0
Biloma (n=1)	0	0	1	0
HCC (n=6)	6	0	0	0
Liver metastasis (n=3)	3	0	0	0
Cystadenocarcinoma (n=3)	3	0	0	0
ICC (n=2)	2	0	0	0
Combined hepatocellular and cholangiocarcinoma (n=2)	2	0	0	0

Equipment and contrast agent

Two US machines were used in this study depending on the availability. One was an Acuson Sequoia 512 US machine (Siemens Medical Solutions, Mountain View, Calif.) equipped with a 4 V1 vector transducer with frequency range of 1.0–4.0 MHz, in which a contrast-specific imaging mode of contrast pulse sequencing (CPS) was installed. The other was an Aplio XV machine (Toshiba Medical Systems, Tokyo, Japan) equipped with a 375BT convex transducer with a center frequency of 3.75 MHz and the contrast-specific imaging mode was contrast harmonic imaging (CHI). The ultrasound contrast agent (UCA) used in this study was SonoVue (Bracco, Milan, Italy), a sulfur hexafluoride-filled microbubble contrast agent.

US examination

All US and CEUS was performed by three experienced staff radiologists. US was performed in advance to examine the liver thoroughly. After identification of the target lesion, the transducer was kept in a stable position and the imaging mode was shifted to low acoustic power contrast-specific imaging mode. In the contrast-enhanced study, low mechanical index (MI) values were used (ranged from 0.15 to 0.21 for CPS in Acuson Sequoia 512 and from 0.05 to 0.08 for CHI in Aplio XV). Imaging settings, such as gain, depth, and focal zone, were optimized to ensure sufficient tissue cancellation with the maintenance of adequate depth penetration. Subsequently, a volume of 2.4 ml SonoVue (5 mg/ml) was injected into the antecubital vein in a bolus

fashion, followed by a flush of 5 ml of 0.9% normal saline solution. The timer was activated promptly from the beginning of UCA administration and the lesion was observed continuously until the clearance of the UCA from the hepatic parenchyma.

The process of CEUS was classified into arterial (10–20 s to 25–35 s after UCA injection), portal (30–45 s to 120 s), and late (>120 s to the disappearance of bubble) phases [4]. The enhancement of the lesion was compared with peripheral hepatic parenchyma. The enhancement pattern and enhancement extent were referenced to the 2008 guideline by EFSUMB study group [4].

Data analysis

The US and CEUS images were independently analysed by a staff radiologist, who had at least 5 years' experience in liver CEUS and at least 14 years' experience in liver US, and a resident radiologist, who had less than 2 years' experience in liver CEUS and less than 3 years' experience in liver US. Both readers were blinded to patient identification, clinical history, other imaging results, and pathological results.

After review of the US images, a confidence rating score was assigned on the basis of a five-point scale (1, definitely benign; 2, probably benign; 3, indeterminate; 4, probably malignant; 5, definitely malignant) for each lesion by both readers. If a further specific diagnosis could be made to the lesion, it was recorded. The procedure was repeated after adding CEUS for analysis. The diagnostic criteria for each entity were presented in Table 2 [4, 5, 7–12].

Statistical analysis

Receiver operating characteristic (ROC) curves were plotted for evaluating the diagnostic performance of US and CEUS in regard to discrimination between benign and malignant lesions, using the SPSS 13.0 software package (SPSS, Chicago, Ill.). Differences between ROC curves were compared using a univariate *z*-score test. The diagnostic performance was expressed as the area under the ROC curve (Az). The lesions assigned a confidence rating score of 3 or more were regarded as positive results, and those assigned a confidence rating score of 1 or 2 were defined as negative results. Sensitivity, specificity, accuracy, positive predictive value (PPV) and negative predictive

Table 2 Diagnostic criteria for cystic FLLs on BUS and CEUS

Entity	BUS	CEUS
Abscess	Ill-defined, heterogeneous, hypo-echoic cystic mass with thick wall, central fluid-filled areas, posterior acoustic enhancement, often containing septa and debris and sometimes containing gas inside the lesion, no or few internal flow signals.	Thick rim-like hyper-enhancement, with or without hyper-enhanced septa and liver segment. Honeycomb-like hyper-enhancement during the arterial phase; hypo-enhancement during the portal or late phase.
Simple cyst	Anechoic mass with sharp smooth border, thin wall, and posterior acoustic enhancement	Non-enhancement throughout three phases.
Hemangioma	Homogeneous echogenic lesion, echogenic peripheral rim, no or few peripheral or intralesional flow signals	Peripheral nodular enhancement during the arterial phase, partial or complete centripetal filling during the portal and late phases
Hematoma	Ill- or well-defined cystic mass with variable echogenicity, no internal arterial flow signals. Small irregular liver lacerations.	Non-enhancement throughout three phases.
Cystadenoma	Well-defined unilocular or multilocular cystic mass, mural or septal nodules are rare.	Septa enhancement during the arterial phase, hypo-enhancement during the portal and late phases
HCC	Heterogeneous echogenic lesion, hypoechoic rim, peripheral or internal arterial flow signals, liver cirrhosis background	Homogeneous or heterogeneous hyper-enhancement during the arterial phase, hypo-enhancement during the portal and late phases
Liver metastasis	Well-defined heterogeneous echogenic lesion, multiple lesions, obvious hypoechoic halo, target sign, no or few peripheral flow signals, non-cirrhotic liver	Peripheral rim-like hyper-enhancement, variable intra-lesional enhancement during the arterial phase, hypo-enhancement or no enhancement during the portal and late phases
Cystadenocarcinoma	Multilocular cystic mass with mural or septal nodules. Thick and coarse calcifications on the septa.	Septa enhancement during the arterial phase, with mural or septal nodules enhancement; hypo-enhancement during the portal or late phase

value (NPV) were calculated. Differences in sensitivity, specificity, accuracy, and correctly characterized nodules were tested using the McNemar test and that in PPV and NPV were tested by chi-square test or Fisher exact test. Interobserver agreement was assessed by weighted Kappa statistics. The agreement was graded as follows: poor ($\kappa < 0.20$), moderate ($\kappa = 0.20$ to < 0.40), fair ($\kappa = 0.40$ to < 0.60), good ($\kappa = 0.60$ to < 0.80), or very good ($\kappa = 0.80$–1.00). $P < 0.05$ was considered to indicate a statistically significant difference. The statistical analyses were performed using the same SPSS 13.0 software package.

Results

Enhancement features of complex cystic FLLs

Benign complex cystic FLLs

For the 29 pyogenic abscesses, 23 (79.3%) showed hyper-enhancement in the arterial phase, which became iso- ($n=8$) or hypo-enhancement ($n=15$) in the late phase. The remaining six (20.7%) lesions showed iso-enhancement in the arterial phase and hypo-enhancement in the late phase. Twenty-six (89.7%) lesions were irregularly rim-like enhanced and three (10.3%) lesions honeycomb-like enhanced, with complete non-enhanced areas in the lesions. Seventeen in 26 rim-like enhanced lesions showed enhanced septa (Fig. 1).

Peripheral nodular hyper-enhancement in the arterial phase and centripetal filling enhancement in the portal and late phases were seen in all the five hemangiomas, and non-enhanced areas were present in the center throughout three phases (Fig. 2).

Complete non-enhancement throughout three phases was displayed in five hepatic cysts (Fig. 3), four hematomas, one intrahepatic cystic cholangiectasis, one cyst-like lesion, and one parasitic liver cyst.

Hyper-enhanced septa in the arterial phase were displayed in two cystadenomas and one vascular hemangioma, with complete non-enhanced areas between septa. In the portal and late phases, the enhancement of the septa

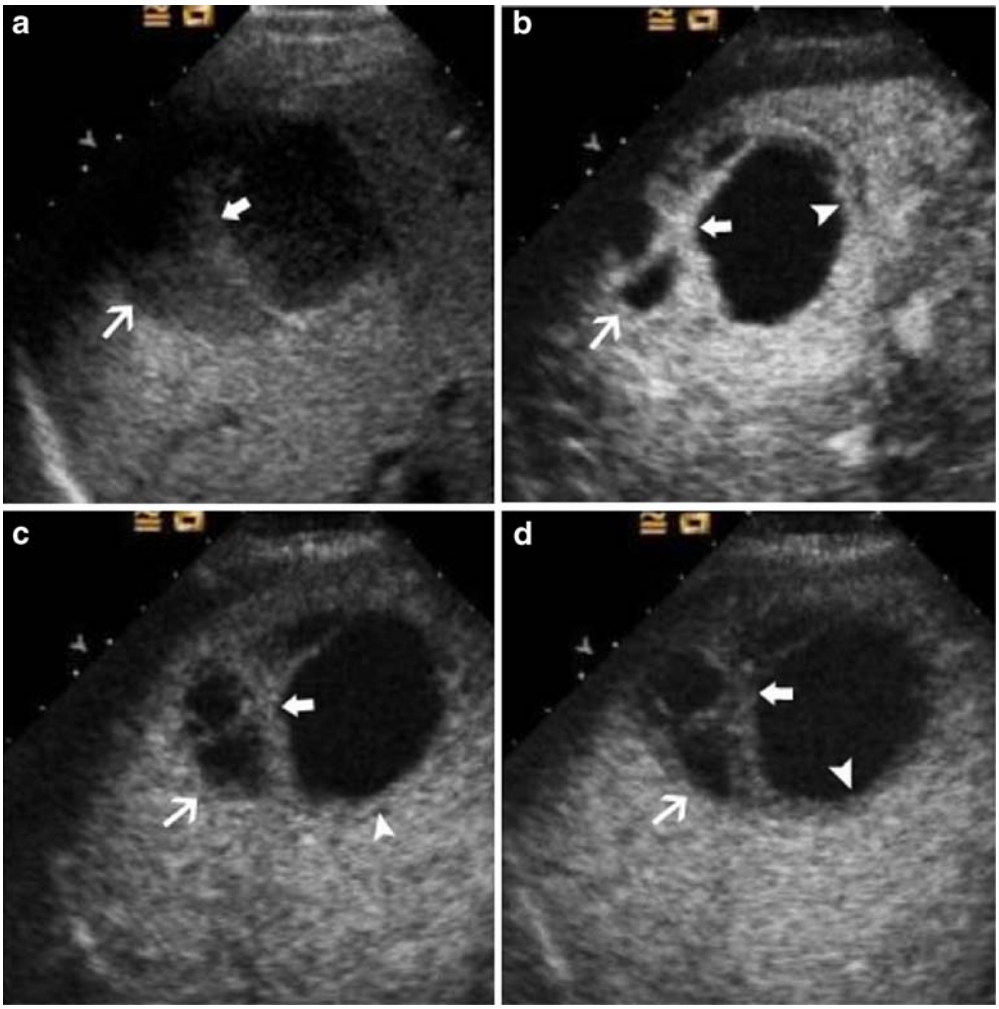

Fig. 1 Pyogenic abscess in a 44-year-old man. **a** US shows a hypo-echoic cystic mass (*thin arrow*) sized 6.6 cm in diameter (*bold arrow* indicates the septa). **b–d** Serial contrast-enhanced images obtained 25 s (**b**), 109 s (**c**), 240 s (**d**) after UCA injection show rim-like (*arrowhead*) enhanced lesion (*thin arrow*) with enhanced septa (*bold arrow*) in the arterial phase **(b)** and the enhancement become hypo-enhancement 109 s after UCA injection (**c**)

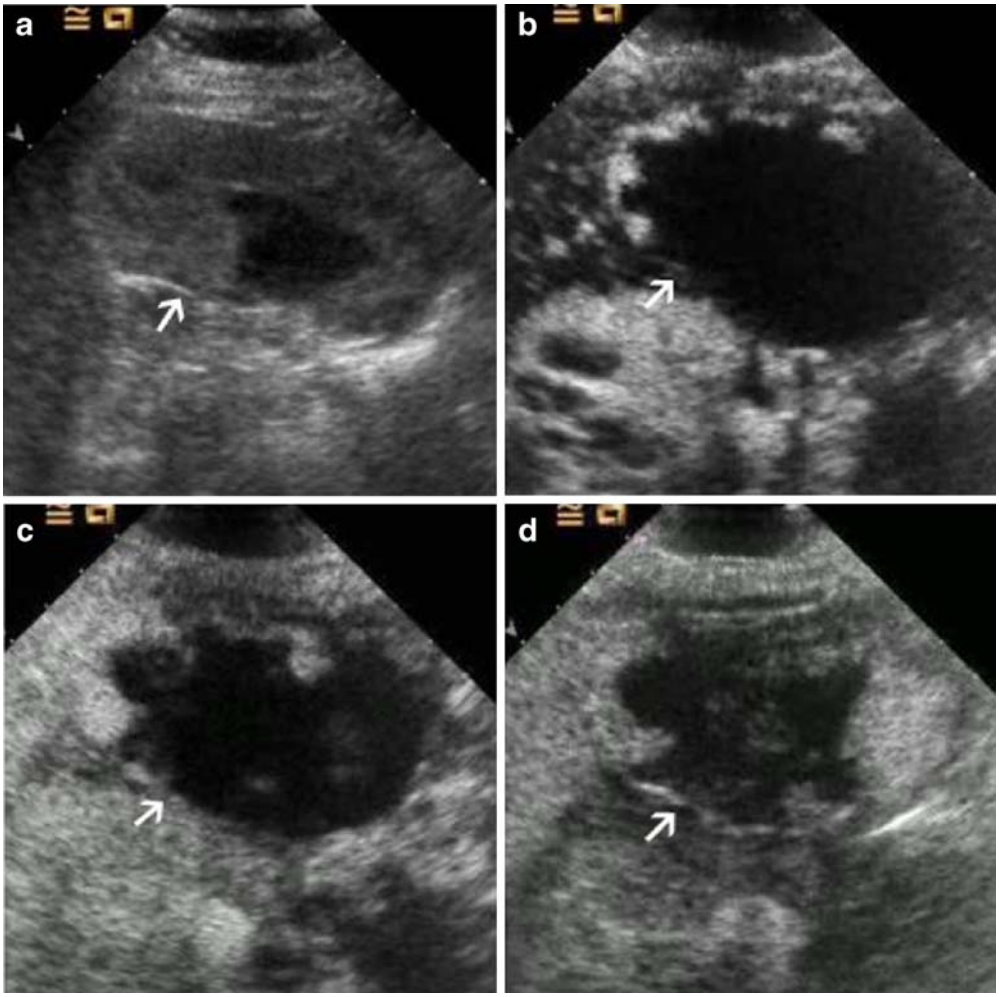

Fig. 2 Hemangioma in a 57-year-old woman. **a** US shows a heterogeneous hypo-echoic cystic mass (*arrow*) sized 7.0 cm in diameter in segment 6. **b–d** Serial contrast-enhanced images obtained 16 s (**b**), 43 s (**c**), 184 s (**d**) after UCA injection show peripheral nodular hyper-enhancement in the arterial phase (**b**) and centripetal filling enhancement in the portal and late phases (**c**, **d**)

became iso-enhancement in one cystadenoma and one vascular hemangioma, and hypo-enhancement in one cystadenoma (Fig. 4).

Slowly stepwise hypo-enhancement of the mural nodules in the arterial phase and sustained hypo-enhancement in the portal and late phases were displayed in one biloma, with complete non-enhanced central area throughout three phases.

Rim-like hyper-enhancement in the arterial phase and hypo-enhancement in the portal and late phases were displayed in one infectious granuloma-like lesion (Table 3).

Two cystadnocarcinomas displayed mural nodule-like hyper-enhancement and non-enhanced central area in the arterial phase, and the remaining one lesion showed hyper-enhancement of septa (Fig. 5).

One intrahepatic cholangiocarcinoma showed irregular peripheral hyper-enhancement with thick and coarse enhanced septa and the other showed honeycomb-like hyper-enhancement in the arterial phase.

During portal and late phases, the hyper-enhanced areas in all the malignant complex cystic FLLs washed out and showed hypo-enhancement (Table 3).

Malignant complex cystic FLLs

All the six HCCs, three metastases and two combined hepatocellular cholangiocarcinomas exhibited irregularly peripheral hyper-enhancement with complete non-enhanced areas in the arterial phase. Two HCCs and two metastases had thick, coarse enhanced septa, whereas none of the combined hepatocellular cholangiocarcinoma showed enhanced septa.

Confidence level and interobserver agreement

The confidence levels for both readers were presented in Table 4. After CEUS, the number of the indeterminate lesions (i.e., assigned confidence rating score 3) decreased, whereas the number of definite lesions (i.e., assigned confidence rating score 1 or 5) increased for both readers. The interobserver agreement also increased from 0.325 (95% confidence interval: 0.214–0.436) to

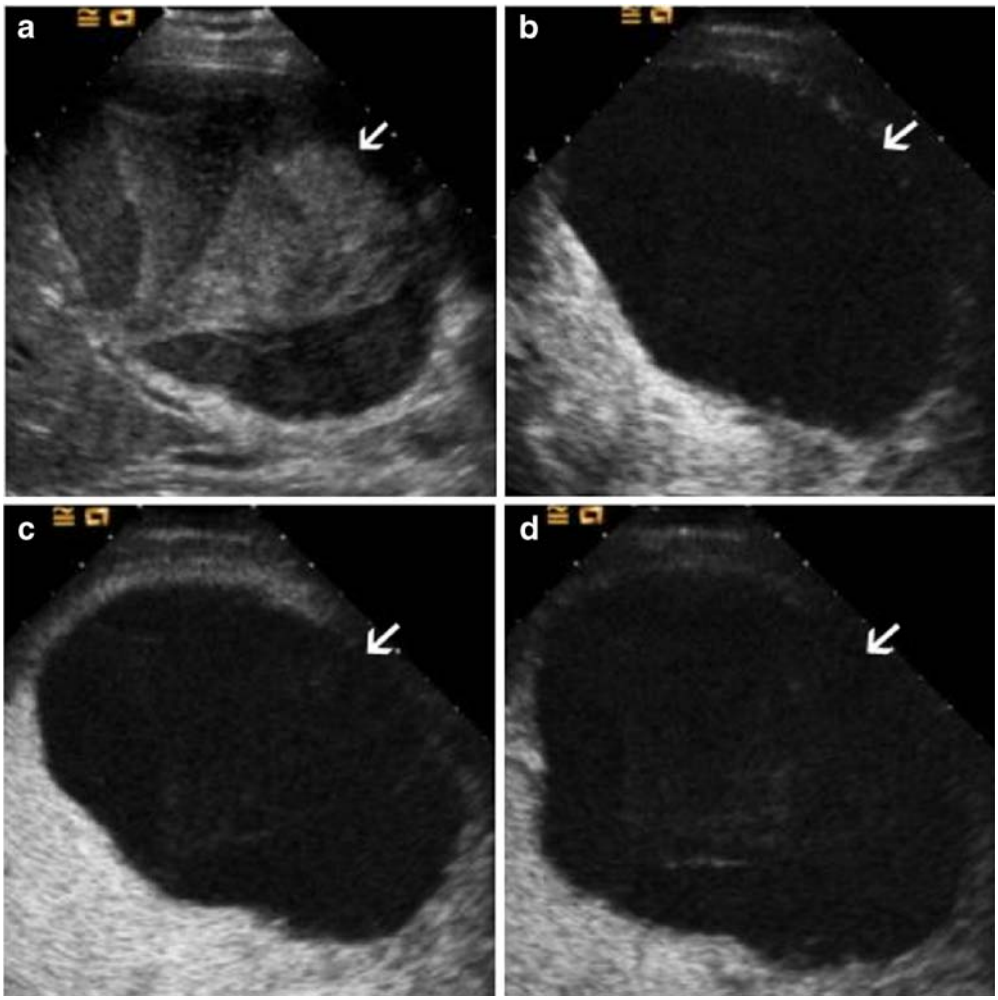

Fig. 3 Hepatic cyst complicated with intracystic hemorrhage in a 57-year-old woman. **a** US shows a well-defined heterogeneous echoic mass (*arrow*) sized 12.5 cm in diameter. **b–d** Serial contrast-enhanced images obtained 15 s (**b**), 55 s (**c**), 182 s (**d**) after UCA injection show complete non-enhancement throughout three phases

0.774 (95% confidence interval: 0.688–0.860) after CEUS.

ROC analysis

The areas under the ROC curve (Az) were 0.774 before versus 0.922 after CEUS in the resident radiologist (P=0.047) and 0.917 versus 0.935 in the staff radiologist (P=0.38, Fig. 6). A significant difference in Az between the resident radiologist and the staff radiologist was found for US (0.774 versus 0.917, P=0.044), whereas not found for CEUS (0.922 versus 0.935, P=0.42). For both readers, the specificity, PPV, and accuracy improved after CEUS (all P<0.05), whereas no improvement was found for sensitivity and NPV (all P>0.05, Table 5).

Specific diagnosis

The percentages of the correctly characterized lesions (i.e., specifically diagnosed lesions) were 28.4% (19/67) before versus 58.2% (39/67) after CEUS (P<0.001) for the resident radiologist, and 26.9% (18/67) versus 76.1% (51/67) for the staff radiologist (P<0.001).

Both readers were failed to characterize five hemangiomas on US, whereas they made the correct diagnosis in all with CEUS. The number of correctly characterized lesions also increased in most of other entities (abscess, HCC, hepatic cyst, hematoma, cystadenoma and cystadenocarcinoma) with the aid of CEUS. Conversely, for the three liver metastases, both readers were unable to make correct diagnosis before and after CEUS (Table 6).

Discussion

Complex cystic FLLs can be classified as developmental, inflammatory, neoplastic and miscellaneous types [13]. Benign complex cystic FLLs include all developmental (e.g., simple cyst), inflammatory (e.g., abscess, parasitic liver cyst) and miscellaneous (e.g., hematoma, biloma) lesions and some neoplastic lesions (e.g., cavernous hemangioma, biliary cystadenoma). Malignant complex

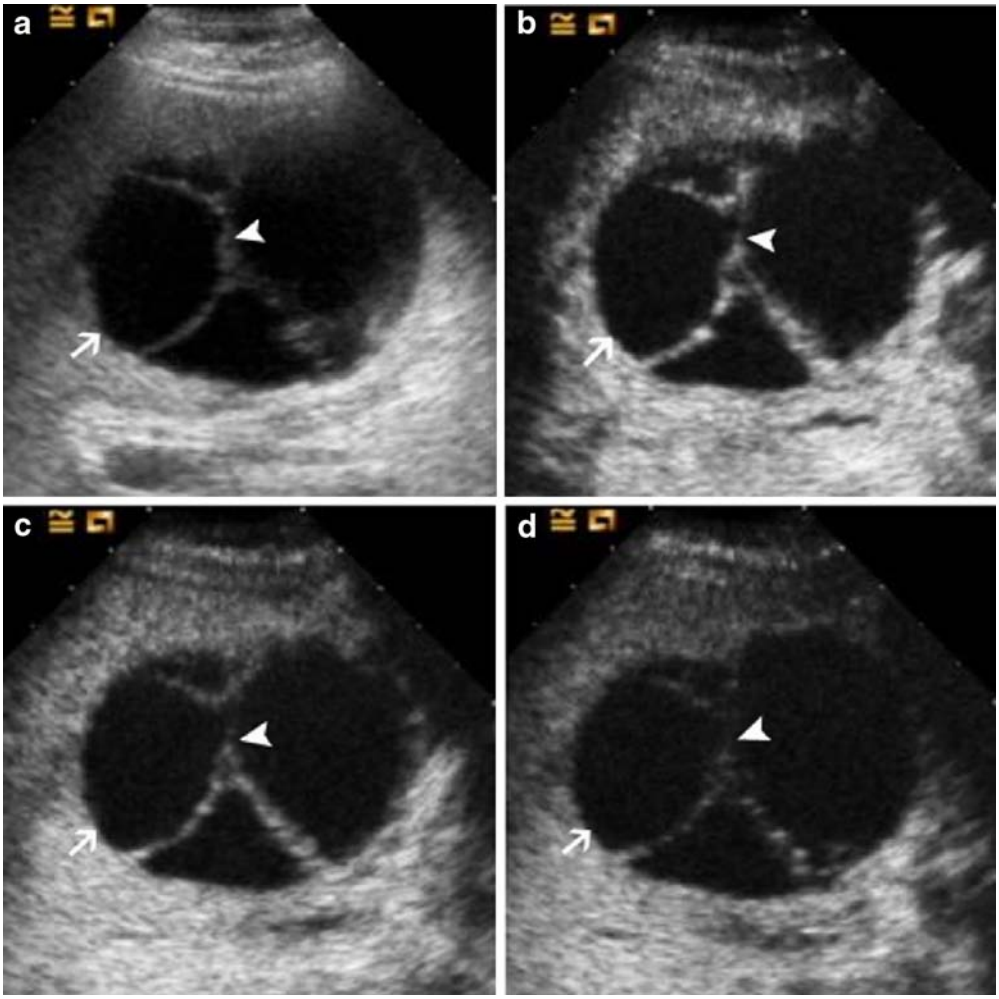

Fig. 4 Cystadenoma in a 44-year-old woman. **a** US shows a well-defined cystic mass (*arrow*) with septa (*arrowhead*) sized 11.6 cm in diameter in segment 4. **b–d** Serial contrast-enhanced images obtained 14 s (**b**), 53 s (**c**), 138 s (**d**) after UCA injection show hyper-enhanced septa in the arterial phase (**b**, *arrowhead*) and the enhancement become hypo-enhancement (*arrowhead*) 53 s after UCA injection (**c**)

cystic FLLs generally include HCC, cystic liver metastasis, and cystadenocarcinoma. The differentiation between benign and malignant lesions is extremely important because the treatment strategies for them vary tremendously [13–15].

Although US has been regarded as the first-line modality for hepatic imaging, its diagnostic ability is limited in most complex cystic FLLs. For instance, a simple cyst complicated with intracystic hemorrhage has a similar manifestation to a cystic neoplasm on US [1, 2]. Radiologists also have difficulty in differentiating an abscess from HCC or liver metastasis solely depending on the features on US when the abscess has little or no liquor puris in it [3, 16].

CEUS operated at low MI allows dynamic real-time evaluation of both the macrocirculation and microcirculation of FLLs. It has been shown that CEUS can greatly improve the diagnostic accuracy of FLLs compared with US [4–6]. As to complex cystic FLLs, Catalano et al. [8] reported 13 abscesses that showed characteristic CEUS features, including rim enhancement, persistent enhanced septa and transient arterial phase hypervascularity around abscesses. Xu et al. [9] reported a case of cystadenoma that showed hyper-enhancement of the cystic wall, internal septations and intracystic solid portion during the arterial phase and hypo-enhancement during the portal and late phases. Despite this, the diagnostic performance of CEUS for complex cystic FLLs has not yet been extensively evaluated.

In the present study, complete non-enhancement throughout three phases or sustained enhancement in the portal and late phases were exhibited in most benign complex cystic FLLs, with the exception of 21 pyogenic abscesses, one cystadenoma and one infectious granuloma-like lesion. On the other hand, hypo-enhancement in the late phase was seen in all malignant complex cystic FLLs. Therefore, the characterization algorithm of CEUS for solid FLLs (i.e., sustained enhancement in late phase indicates benign lesions and washout in late phase indicates malignancies) [6] is also applicable for most complex cystic FLLs.

With regard to discrimination between benign and malignant lesions, significant improvement in Az was found for the resident radiologist after CEUS, whereas not

Table 3 The enhancement features of cystic FLLs

Enhancement feature			Benign lesions					*Malignant lesions*			
			Abscess (n=29)	Hemangioma (n=5)	Cyst (n=5)	Hematoma (n=4)	Cystadenoma (n=2)	HCC (n=6)	Metastasis (n=3)	Cystadenocarcinoma (n=3)	Combined hepatocellular cholangiocarcinomas (n=2)
Enhancement pattern[a]		I	0	0	0	0	2	0	0	1	0
		II	26	0	0	0	0	0	0	0	0
		III	3	0	0	0	0	0	0	0	0
		IV	0	5	0	0	0	0	0	0	0
		V	0	0	0	0	0	0	0	2	0
		VI	0	0	5	4	0	0	0	0	0
		VII	0	0	0	0	0	6	3	0	2
Enhancement extent	Arterial	Hyper	23	5	0	0	2	6	3	3	2
		Iso	6	0	0	0	0	0	0	0	0
		Hypo	0	0	0	0	0	0	0	0	0
		Non	0	0	5	4	0	0	0	0	0
	Portal/ late	Hyper	0	1	0	0	0	0	0	0	0
		Iso	8	4	0	0	1	0	0	0	0
		Hypo	21	0	0	0	1	6	3	3	2
		Non	0	0	5	4	0	0	0	0	0

[a] *I* septate enhancement (i.e., enhancement of septa), *II* rim-like enhancement, *III* honeycomb-like enhancement, *IV* peripheral nodular enhancement, *V* mural nodules enhancement, *VI* no enhancement, *VII* peripheral enhancement

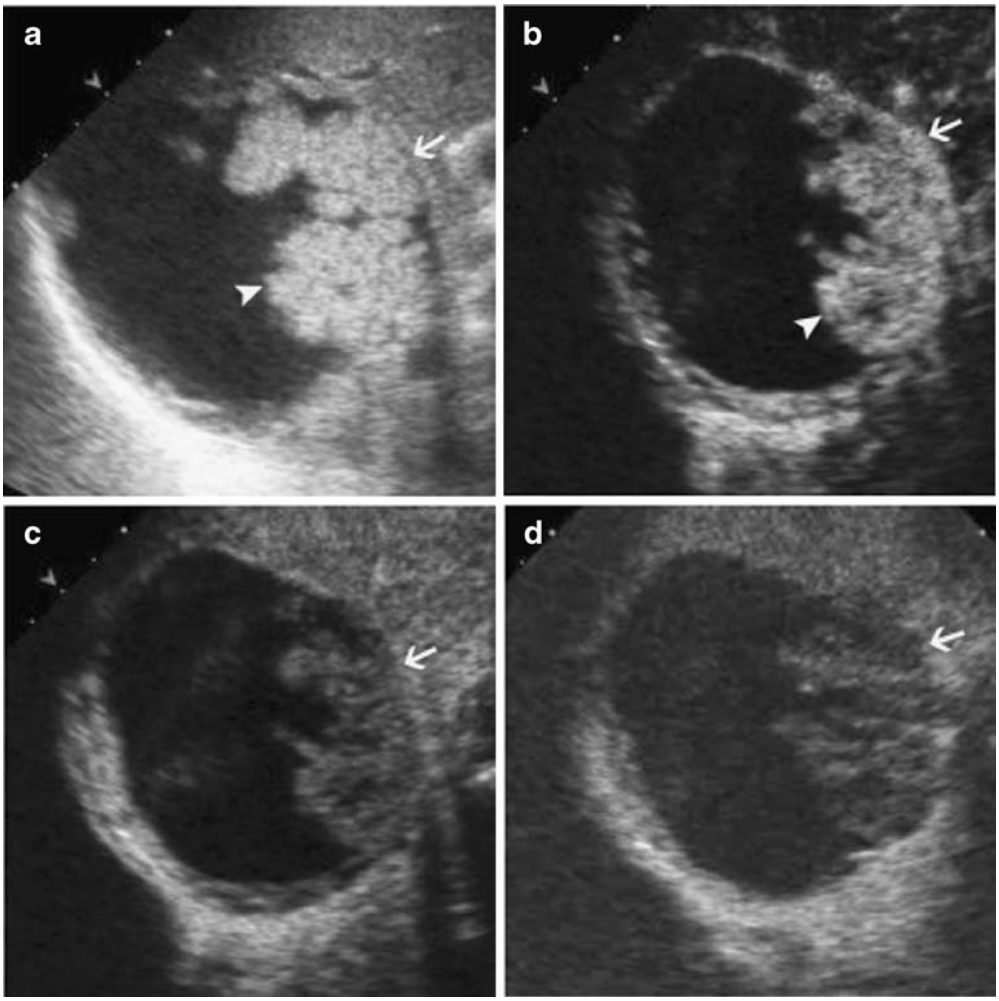

Fig. 5 Cystadenocarcinoma in a 50-year-old woman. **a** US shows a well-defined cystic mass (*arrow*) with mural nodules (*arrowhead*) sized 8.9 cm in diameter. **b–d** Serial contrast-enhanced images obtained 14 s (**b**), 41 s (**c**), 169 s (**d**) after UCA injection show mural nodule-like hyper-enhancement (*arrowhead*) and non-enhanced central area in the arterial phase (**b**) and the enhancement become hypo-enhancement 41 s after UCA injection (**c**)

found for the staff radiologist, in whom both US and CEUS obtained satisfactory diagnostic results. On the other hand, a significant difference in Az between the resident and the staff radiologists was found on US but not found on CEUS. This phenomenon indicates that for the resident radiologist, it requires a long learning process to obtain the similar diagnostic performance as the staff radiologist on US. Nevertheless, with the help of CEUS, this process will be greatly shortened since both the resident and the staff radiologists had similar results in Az on CEUS. In other words, CEUS will change the learning curve in diagnosing complex cystic FLLs. The improved interobserver agreement after CEUS also supported this hypothesis.

As to specific diagnosis, CEUS greatly improved the ability in defining the natures of the complex cystic FLLs in both the resident and staff radiologists, compared with US. CEUS is particularly useful in the characterization of some non-neoplastic lesions, such as pyogenic abscess,

Table 4 The numbers of lesions with an assigned confidence rating score in 67 cystic FLLs

US	Reader	Assigned confidence rating score[a]				
		1	2	3	4	5
BUS	Resident	2 (3.0%)	26 (38.8%)	24 (35.8%)	14 (20.9%)	1 (1.5%)
	Staff	19 (28.4%)	18 (26.9%)	20 (29.8%)	9 (13.4%)	1 (1.5%)
CEUS	Resident	35 (52.2%)	11 (16.4%)	1 (1.5%)	5 (7.5%)	15 (22.4%)
	Staff	52 (77.5%)	0 (0.0%)	3 (4.5%)	6 (9.0%)	6 (9.0%)

[a] *1* definitely benign; *2* probably benign; *3* indeterminate; *4* probably malignant; and *5* definitely malignant

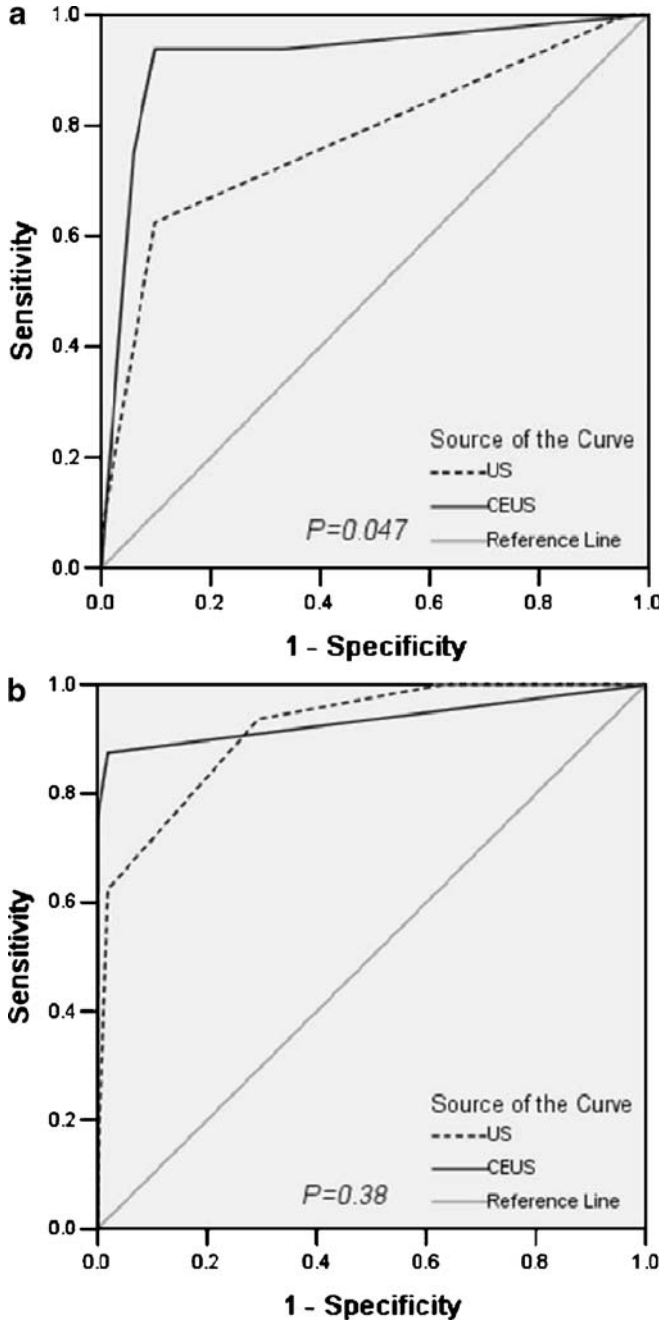

Fig. 6 ROC curves before (US) and after (CEUS) review of CEUS images for the resident (**a**) and the staff radiologists (**b**)

hemangioma, hepatic cyst, and hematoma. A pyogenic abscess always shows a characteristic rim-like or honeycomb-like enhanced pattern in the arterial phase. Cystic hemangioma also shows the same typical peripheral nodular enhancement as its solid counterpart. Hepatic cyst and hematoma exhibit non-enhancement throughout three phases so that it was convenient to differentiate them from cystic neoplasms. In this study, characteristic features displayed on CEUS of some pyogenic abscesses directly prompted US-

Table 5 Diagnostic performance in differentiating the malignant cystic focal liver lesions from the benign ones before and after review of CEUS images

Reader	Performance parameter	Total (n=67)		
		Before	After	P
Resident radiologist	Az	0.774 (0.626–0.922)	0.922 (0.832–1.011)	0.047[a]
	Sensitivity, %	81.3% (13/16)	93.8% (15/16)	0.500
	Specificity, %	47.1% (24/51)	88.2% (45/51)	0.000[a]
	PPV, %	32.5% (13/40)	71.4% (15/21)	0.006[a]
	NPV, %	88.9% (24/27)	97.8% (44/45)	0.140
	Accuracy, %	55.2% (37/67)	89.6% (60/67)	0.000[a]
Staff radiologist	Az	0.917 (0.842–0.991)	0.935 (0.838–1.032)	0.380
	Sensitivity, %	93.8% (15/16)	87.5% (14/16)	1.000
	Specificity, %	70.6% (36/51)	98.0% (50/51)	0.001[a]
	PPV, %	50.0% (15/30)	93.3% (14/15)	0.007[a]
	NPV, %	97.3% (36/37)	96.2% (50/52)	1.000
	Accuracy, %	76.1% (51/67)	97.0% (65/67)	0.004[a]

Numbers in parentheses for Az are 95% confidence intervals; *numbers in parentheses for other parameters* are numbers of the lesions used to calculate the percentages
[a]Statistically significant difference

Table 6 Results of specific diagnosis in the cystic FLLs before and after review of CEUS images (*Met* liver metastasis, *Ind* indeterminate)

Reader	Entity	CEUS	Results of specific diagnosis								
			Abscess	Cyst	Hemangioma	Hematoma	Cystadenoma	HCC	Met	Cystadenocarcinoma	Ind
Staff radiologist	Abscess (n=29)	Before	14	0	1	0	0	0	0	0	14
		After	29	0	0	0	0	0	0	0	0
	Hepatic cyst (n=5)	Before	0	1	0	0	0	0	0	0	4
		After	0	5	0	0	0	0	0	0	0
	Hemangioma (n=5)	Before	0	0	0	0	0	0	0	0	5
		After	0	0	5	0	0	0	0	0	0
	Hematoma (n=4)	Before	1	0	0	0	0	0	0	0	3
		After	0	1	0	2	0	0	0	0	1
	Cystadenoma (n=2)	Before	0	1	0	0	0	0	0	0	1
		After	0	0	0	0	2	0	0	0	0
	HCC (n=6)	Before	0	0	1	0	0	2	0	0	3
		After	0	0	0	0	1	5	0	0	0
	Met (n=3)	Before	0	0	0	0	0	1	0	0	2
		After	1	0	0	0	0	1	0	0	1
	Cystadenocarcinoma (n=3)	Before	0	0	0	0	0	1	0	2	0
		After	0	0	0	0	0	0	0	3	0
Resident radiologist	Abscess (n=29)	Before	14	0	0	0	0	0	0	0	15
		After	21	0	0	0	3	3	1	0	1
	Hepatic cyst (n=5)	Before	0	1	0	0	0	0	0	0	4
		After	0	3	0	0	2	0	0	0	0
	Hemangioma (n=5)	Before	0	0	0	0	0	0	1	0	4
		After	0	0	5	0	0	0	0	0	0
	Hematoma (n=4)	Before	0	0	0	0	0	0	0	0	4
		After	2	1	0	0	0	0	0	1	0
	Cystadenoma (n=2)	Before	0	0	0	0	2	0	0	0	0
		After	0	0	0	0	2	0	0	0	0
	HCC (n=6)	Before	0	0	0	0	0	2	1	0	3
		After	0	0	0	0	0	0	6	0	0
	Met (n=3)	Before	0	0	0	0	0	1	0	0	2
		After	1	0	0	0	0	2	0	0	0
	Cystadenocarcinoma (n=3)	Before	0	0	0	0	0	2	0	1	0
		After	0	0	0	0	0	1	0	2	0

guided percutaneous aspiration and drainage, avoiding further CECT or CEMR examination. With the help of CEUS, both readers made correct diagnosis in most neoplastic lesions, such as HCC, cystadenoma, and cystadenocarcinoma, because of the characteristic enhancement patterns as described before [4, 9–11, 13]. Conversely, it was unexpected that both readers made wrong specific diagnoses in all the three cystic metastases on CEUS, largely due to anonymity to the patient history and other imaging studies.

In the present study, the number of the malignant complex cystic FLLs was less than that of the benign lesions, which would lead to selection bias. The disparity in entity composition may reflect the disparity of incidence between benign and malignant lesions, since benign complex cystic FLLs are much more common than malignant. Another limitation was that CEUS images were reviewed immediately after US images in each case, which might cause observer bias. Though this method is not strictly appropriate, it is reasonable and acceptable in clinical practice, since the investigators have to refer to US to determine the target lesion before CEUS.

Conclusions

CEUS with low MI techniques and a second-generation contrast agent improves the capability of discrimination

between benign and malignant complex cystic FLLs, especially for resident radiologists. CEUS also increases the interobserver agreement in characterization for complex cystic FLLs in comparison with US.

Acknowledgements This work was supported in part by grant 30300082 and 30470467 from National Scientific Foundation Committee of China, and grant NCET-06-0723 from Chinese Ministry of Education.

References

1. Hagiwara A, Inoue Y, Shutoh T et al (2001) Haemorrhagic hepatic cyst: a differential diagnosis of cystic tumour. Br J Radiol 74:270–272
2. Kitajima Y, Okayama Y, Hirai M et al (2003) Intracystic hemorrhage of a simple liver cyst mimicking a biliary cystadenocarcinoma. J Gastroenterol 38:190–193
3. Ryan RS, Al-Hashimi H, Lee MJ (2001) Hepatic abscesses in elderly patients mimicking metastatic disease. Ir J Med Sci 170:251–253
4. Claudon M, Cosgrove D, Albrecht T et al (2008) Guidelines and good clinical practice recommendations for the contrast enhanced ultrasound (CEUS)-update 2008. Ultraschall Med 29:28–44
5. Xu HX, Liu GJ, Lu MD et al (2006) Characterization of small focal liver lesions using real-time contrast-enhanced sonography: diagnostic performance analysis in 200 patients. J Ultrasound Med 25:349–361
6. Quaia E, Caliada F, Bertolotto M et al (2004) Characterization of focal liver lesions with contrast-specific US modes and a sulfur hexafluoride-filled microbubble contrast agent: diagnostic performance and confidence. Radiology 232:420–430
7. Xu HX, Lu MD, Liu GJ et al (2006) Imaging of peripheral cholangiocarcinoma with low-mechanical index contrast-enhanced sonography and SonoVue:initial experience. J Ultrasound Med 25:23–33
8. Catalano O, Sandomenico F, Raso MM et al (2004) Low mechanical index contrast-enhanced sonographic findings of pyogenic hepatic abscesses. AJR Am J Roentgenol 182:447–450
9. Xu HX, Xie XY, Lu MD et al (2008) Unusual benign focal liver lesions: findings on real-time contrast-enhanced sonography. J Ultrasound Med 27:243–254
10. Korobkin M, Stephens DH, Lee JK et al (1989) Biliary cystadenoma and cystadenocarcinoma: CT and sonographic findings. AJR Am J Roentgenol 153:507–511
11. Federle MP, Filly RA, Moss AA (1981) Cystic hepatic neoplasms: complementary roles of CT and sonography. AJR Am J Roentgenol 136:345–348
12. Spiegel RM, King DL, Green WM (1978) Ultrasonography of primary cysts of the liver. AJR Am J Roentgenol 131:235–238
13. Mortelé KJ, Ros PR (2001) Cystic focal liver lesions in the adult: differential CT and MR imaging features. Radiographics 21:895–910
14. Teoh AY, Ng SS, Lee KF et al (2006) Biliary cystadenoma and other complicated cystic lesions of the liver: diagnostic and therapeutic challenges. World J Surg 30:1560–1566
15. Ammori BJ, Jenkins BL, Lim PC et al (2002) Surgical strategy for cystic diseases of the liver in a western hepatobiliary center. World J Surg 26:462–469
16. N'Gbesso RD, Attia A, Mahassadi A et al (1998) Hepatocellular carcinoma (HCC) observed in Abidjan: aspects and role of ultrasonography. J Radiol 79:409–414